

# Crack initiation mechanism of extruded AZ31 magnesium alloy in the very high cycle fatigue regime

F. Yang\*, S.M. Yin, S.X. Li, Z.F. Zhang

*Shenyang National Laboratory for Materials Science, Institute of Metal Research,  
Chinese Academy of Sciences, Shenyang, 110016, PR China*

Received 8 November 2007; received in revised form 21 January 2008; accepted 4 February 2008

## Abstract

Ultrasonic fatigue testing as well as conventional fatigue testing has been conducted on commercial extruded AZ31 magnesium alloy. The *S–N* curve for this alloy appears to have a continuous decreasing trend in the very high cycle regime. Fatigue strength at  $10^9$  cycles is  $88.7 \pm 4.1$  MPa. The ratio of endurance limit at one billion cycles to the tensile strength ( $\sigma_{-1}/\sigma_b$ ) is 0.301. Fatigue failure mainly originated from the specimen surface or near surface, where deformation twins were found after cyclic loading. Fatigue cracks were observed along twin bands. Based on cyclic deformation irreversibility caused by twinning, fatigue damage mechanisms are proposed in terms of surface/near surface crack initiation. © 2008 Elsevier B.V. All rights reserved.

*Keywords:* Magnesium alloy; Ultrasonic fatigue; Crack initiation; Deformation twins; Very high cycle fatigue; Cyclic deformation irreversibility

## 1. Introduction

Weight reduction components have attracted much attention for their economical benefits in terms of energy consumption. In that case, magnesium alloys have received more and more concerns due to their excellent properties, such as low density, high specific strength and stiffness, good machinability, etc. [1,2]. Structural parts of the engine, power transmission and car-body may be made of magnesium alloys [3]. During their life time, some of the components have to survive more than  $10^8$  cycles. Therefore, the study of very high cycle fatigue (number of cycles  $> 10^8$ ) properties of magnesium alloys is of great interest.

For casting magnesium alloys, defects such as casting porosity and cavity may act as crack initiation sites and will have detrimental influences on the material's fatigue behavior [4]. In contrast, wrought alloys have superior fatigue properties because they have no such casting defects [5]. Therefore, using wrought magnesium alloys for research may shed light on the intrinsic fatigue mechanisms of these alloys.

Previous works [5–7] on high cycle fatigue behaviors of wrought magnesium alloys have proposed different crack initiation mechanisms. For the explanation of surface crack initiation, a model of cyclic slip deformation [7] was suggested, while for subsurface crack initiation, a model based on the interaction between single slip and the environment [5] was proposed. Both models have provided reasonable mechanisms for fatigue crack initiation in the alloys investigated by these authors; however, these models might not be applied directly in the present alloy since the cyclic slip conditions for different alloys were not the same and the corrosion properties for different magnesium alloys were different either [8]. On the other hand, it is well known that magnesium has a hexagonal close-packed (hcp) crystal structure which leads to its unique mechanical responses due to the activation of different deformation modes such as basal slip and  $\{10\bar{1}2\}$  twinning [9,10]. But to the author's knowledge, in the very high cycle fatigue regime there has not been a fatigue failure mechanism which has taken into account the specific deformation mechanism in magnesium alloys.

In the present study, very high cycle fatigue behaviors of commercial extruded AZ31 magnesium alloy were examined using ultrasonic fatigue testing machine. In addition, conventional servo-hydraulic fatigue testing was also conducted in the same stress range as that of ultrasonic fatigue for comparison. Based on the experimental observations and the principle

\* Corresponding author. Tel.: +86 24 83978270.  
E-mail address: fanyang@imr.ac.cn (F. Yang).

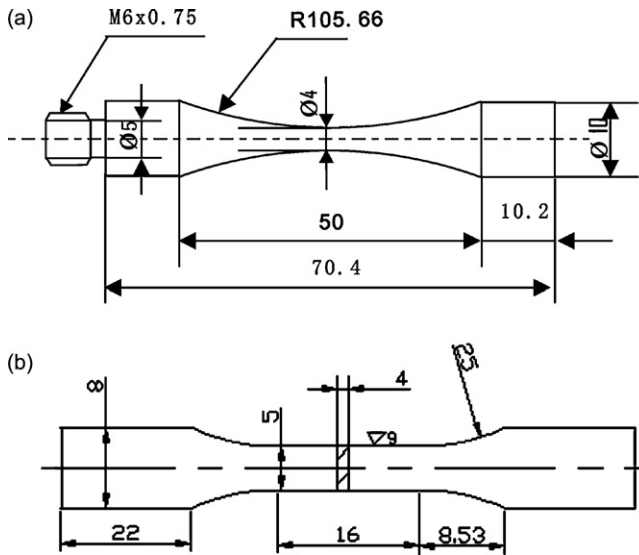


Fig. 1. Specimen shape and dimensions for (a) ultrasonic fatigue testing (round specimen) and (b) conventional fatigue testing (plate specimen), respectively.

of cyclic deformation irreversibility, some explanations were proposed to illustrate the mechanisms of surface/near surface fatigue crack initiation.

## 2. Materials and experimental procedure

The AZ31 (Al 2.9, Zn 1.0, Mn 0.3, balanced Mg by weight%) bars used in our experiment were processed by extrusion with a reduction ratio of 20:1. The  $\{0002\}$  pole figure of this alloy was obtained using X-ray diffraction analysis. Mechanical and fatigue testing specimens were machined with the loading axis parallel to their extrusion directions. The mechanical properties under monotonic loadings are shown in Table 1. Notice that the compressive yield strength (CYS) is obviously lower than the tensile yield strength (TYS); in other words, there is a severe tension–compression yield asymmetry for this alloy.

The dimensions of the specimens for ultrasonic and conventional fatigue tests are shown in Fig. 1. Both tests were performed at room temperature and in ambient air. Ultrasonic fatigue testing was conducted on Shimadzu USF-2000 testing system with a resonance frequency of 20 kHz, a resonance interval of 150 ms and a stress ratio of  $R = -1$ . Specimens were polished by emery paper and then buff-finished before fatigue testing. During the ultrasonic fatigue testing process, specimens were cooled by compressed air and were cycled at constant stress amplitude to  $10^9$  cycles except failure. Some specimens were then cut along the direction parallel to the gage length and prepared for optical microscope observation. Details of ultrasonic fatigue testing procedures and systems are described elsewhere [11]. Conventional servo-hydraulic fatigue testing was conducted on Instron 8871 fatigue testing machine with a frequency of 1 Hz and a load ratio of  $R = -1$ . Electro-polished plate specimens were prepared for the purpose of surface observation. Specimens were first loaded under the stress amplitude of 90 MPa (in the stress range of ultrasonic fatigue loading) for  $10^4$  cycles without failure. After surface analysis, these specimens were further cycled

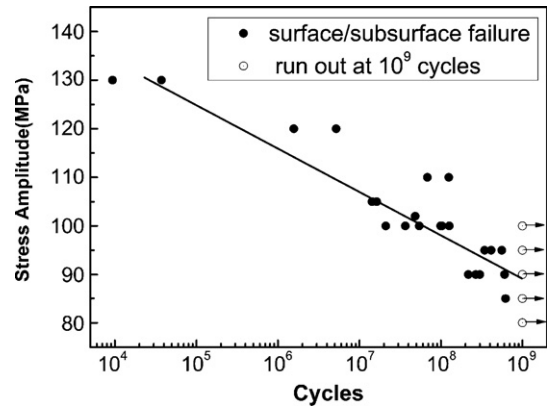


Fig. 2.  $S-N$  curve for AZ31 alloy after ultrasonic fatigue testing.

under higher stress amplitudes in order to speed up the fatigue damage process. Scanning electron microscope (SEM) analysis was conducted with FEI QUANTA-600 SEM equipment.

## 3. Results and discussion

The ultrasonic fatigue  $S-N$  curve is shown in Fig. 2 with a spanned cycle range of  $10^4$ – $10^9$ . Fatigue failures can be observed over most of the testing stress amplitude range and the  $S-N$  curve appears to have a continuous decreasing trend without a horizontal asymptote. Endurance limit of this alloy at  $10^9$  cycles is  $88.7 \pm 4.1$  MPa. Ogarrevic and Stephens [12] have indicated that fatigue ratio ( $\sigma_{-1}/\sigma_b$ ) was between 0.25 and 0.5 for wrought Mg alloys and higher ratios were for higher strength alloys. Here the fatigue ratio for AZ31 alloy at  $10^9$  cycles is 0.301, indicating this alloy has relatively moderate fatigue strength. It was observed that fatigue failure mainly originated from the surface (Fig. 3(a and b)) or slightly below the surface (Fig. 3(c and d)) of the specimens. As a matter of fact these two features are hard to be distinguished from each other in the present work (see Fig. 3), so they are not treated separately in the following discussion and crack initiation from slightly below the specimen surface is referred to as near surface crack initiation.

It has been indicated that crack initiation period may take up more than 90% of the total fatigue life in the very high cycle regime [13], thus emphases were put on the study of crack initiation mechanism [5,7]. From the basic point of view, fatigue failure originates from cyclic deformation irreversibility [14,15]; that is to say, as the fatigue loading goes on, the build up of irreversible deformation may cause local stress concentration and then leads to the initiation of cracks. However, for magnesium alloys, most of the previous works only consider cyclic slip as the cyclic deformation mode. Some authors noticed the environment-assisted cyclic slip irreversibility [5]; some authors concerned about slip bands and the interaction between slip bands and grain boundaries [7]. In our work, the applied AZ31 alloy has superior corrosion resistance due to its higher content of Al and lower content of Zn [8]. Besides, no layer of oxide film as observed in literature [5] has been found in our experiment (see Fig. 3). Thus, only the environmental effects are not enough for the explanation of crack initiation in the present alloy.

Table 1  
Mechanical properties of AZ31 alloy

Material	Tensile yield strength (TYS) (MPa)	Ultimate tensile strength (UTS) (MPa)	Elongation (EL) (%)	Compressive yield strength (CYS) (MPa)
AZ31	187.2	294.5	18.5	89.6

Tensile yield strength (TYS) and compressive yield strength (CYS) are given for 0.2% offset.

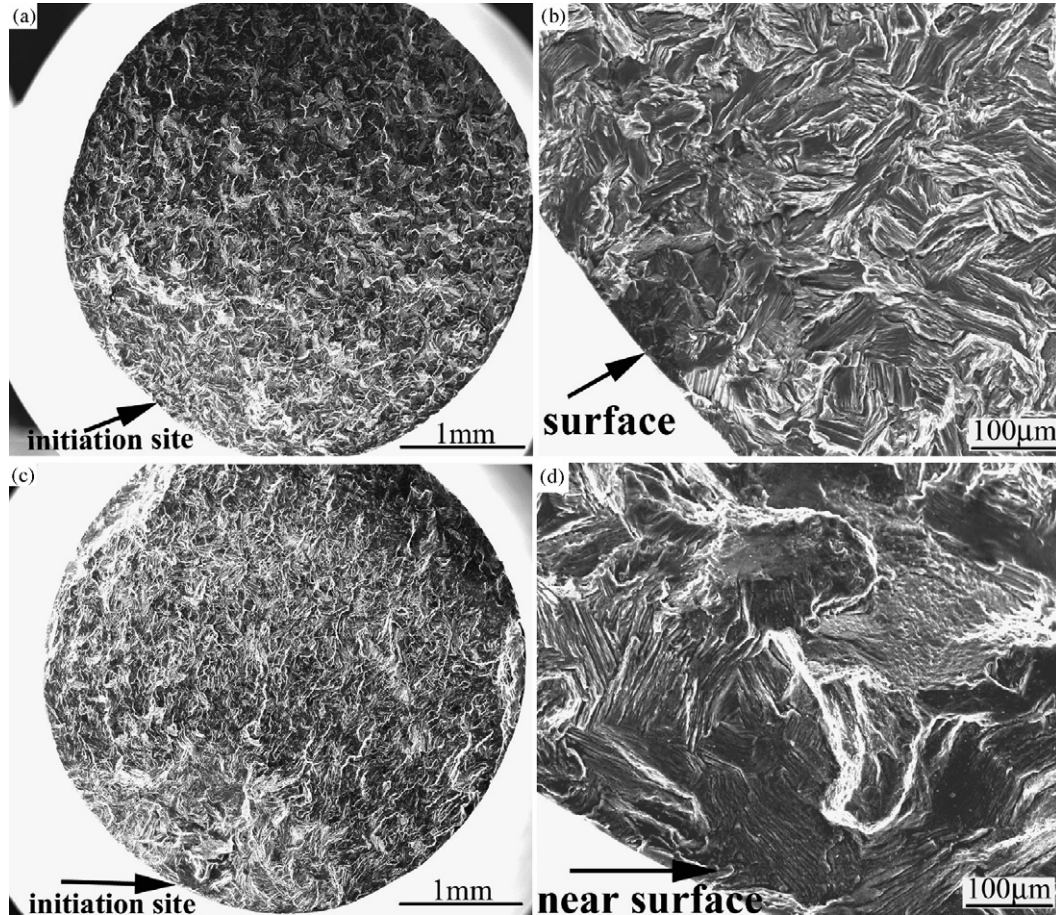


Fig. 3. Low (a and c) and high (b and d) magnification SEM images for fracture surfaces of AZ31 alloy after ultrasonic fatigue loading. Arrows indicate crack initiation from surface (a and b) or from near surface (c and d).

More importantly for hcp-structured magnesium alloys, it is well known that both  $\{0001\}$   $\langle 11\bar{2}0 \rangle$  basal slip and  $\{10\bar{1}2\}$  twinning are the main deformation systems at room temperature [2]. Since the  $\langle 11\bar{2}0 \rangle$  Burgers vector lies in the basal plane, no plastic strain parallel to the  $c$ -axis could be accommodated by this slip system [9]. However, the  $\{10\bar{1}2\}$  twinning could cause extension along the  $c$ -axis, which leads to the activation of twinning mode only by tension but not by compression along the  $c$ -axis [9]. For extruded magnesium alloys, it is considered that basal planes tend to align parallel to the extrusion direction [9]. The  $\{0002\}$  pole figure of our alloy (Fig. 4) also confirms that extruded AZ31 alloy has a strong fiber texture with  $\{0001\}$  basal plane distributed parallel to the extrusion direction. Such an orientation favors extensive  $\{10\bar{1}2\}$  twinning under compressive loading, resulting in a relatively lower compressive yield strength, while both the  $\{0001\}$   $\langle 11\bar{2}0 \rangle$  basal slip and the  $\{10\bar{1}2\}$  twinning are difficult to operate under tensile loading, resulting in a relatively higher tensile yield strength [9,16]. In

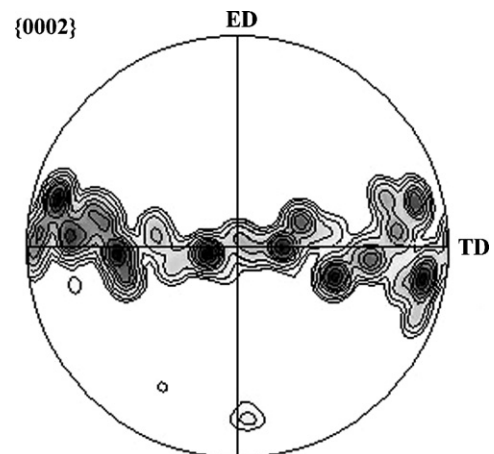


Fig. 4.  $\{0002\}$  pole figure for the extruded AZ31 alloy with ED of the extrusion direction.

our experiment, the applied stress amplitudes (in the range of 80–130 MPa (Fig. 2)) are well below the tensile yield strength 187 MPa (Table 1), so the aforementioned cyclic slip mechanism [7] may not be simply applied in the present condition. In contrast, it is noticed that the compressive yield strength is around 90 MPa (Table 1); so local yielding could exist under most applied stress amplitudes. Therefore, local activation of twinning could be possible during cyclic loading in the very high cycle regime and it could be seen from Fig. 5 that certain amount of deformation twins were formed beneath the fracture surface after fatigue loading. In that case, more attention should be paid on the contribution of deformation twins to the fatigue damage processes.

Fig. 6 shows the microstructures of ultrasonic-fatigued specimen from the section parallel to the gauge length beneath the fracture surface. Arrows in Fig. 6(a) indicate that secondary cracks were formed along twin bands. Fig. 6(b) is the magnified image of the upper crack marked b in Fig. 6(a). For ultrasonic fatigue testing generally running in the very high cycle regime, crack initiation may take up most of the total fatigue life [13]. That is to say, once the crack has initiated, the specimen will break up very soon. Besides, due to the requirements of our ultrasonic fatigue equipment, only round specimens (Fig. 1(a)) were used for this test. Therefore, it is hard to observe crack initiation sites from specimen surfaces in the ultrasonic fatigue test and it is hard to track down the main crack initiation sites from the observation of specimen section parallel to the gauge length as shown in Fig. 6. However, fatigue damage was not just confined on the main cracking layer; thus the observation of secondary cracks beneath the fracture surface could also provide us with a good understanding that twin has played an important role in the process of fatigue crack initiation.

On the other hand, conventional fatigue testing could help us further confirm the crack initiation mechanism. In Fig. 7, surface morphologies for specimen after conventional fatigue loading are shown. After  $10^4$  cycles of fatigue under the stress amplitude of 90 MPa, twins were formed on specimen surface, but cracks have not been seen (Fig. 7(a)), which is reasonable since the life span of  $10^4$  is negligible compared to the general life span of the very high cycle fatigue. Further fatigue loading under the stress amplitude of 120 MPa for several thousand cycles led to crack initiation along some twin bands (Fig. 7(b)). Although ultrasonic fatigue damage process cannot be duplicated simply by conventional fatigue process, the results obtained in Fig. 7 could still reflect that twin has played an important role in crack initiation in the very high cycle fatigue regime.

Twinning-involved fatigue crack initiation has been mentioned by Shih et al. [6], but they did not come up with an explicit description of that process. Here, based on cyclic deformation irreversibility caused by twinning, further description was proposed to illustrate the twinning-involved fatigue damage mechanism. For the cyclic loading in the tension half cycle, both twinning and basal slip were hard to initiate. Testing specimens were undergone just elastic deformation since the tensile loading was much lower than the tensile yield strength. As it went into the compression half cycle, stress amplitude was high enough to activate the  $\{10\bar{1}2\}$  twinning system and local yielding could

take place in the specimen. When the fatigue loading reversed again to tensile stress, some of the twinned regions might disappear due to the mechanism of detwinning [16]. However, the process of detwinning could not be fully reversible [17]; there would be some remaining twins.

In the twinning-involved fatigue damage process, deformation twins could contribute from three aspects. First, although twin boundaries are the plane imperfections with the lowest energy, their roles in crack initiation have long been noticed [18]. The sharp edge of existing twin lamellas could cause local stress concentration [19] and the remaining twin-matrix interfaces could act as preferential sites for crack nucleation as observed in titanium [18]. Second, as fatigue loading went on, the twinning and detwinning processes kept repeating too. But not all of the twinned areas could be retreated during the reverse loading as observed by Stevenson and Vander Sande [17]. Therefore, just like cyclic slip, this cyclic twinning was also a form of plastic deformation and could also lead to certain degree of cyclic deformation irreversibility which is the basic mechanism for fatigue damage. Finally, the contribution of twinning to plastic deformation is not only for its direct shear strain but also for its modification of grain orientation [16] which might favor the initiation of dislocation slip in order to provide further plastic deformation. Since crack initiation stage might take up most of the total fatigue life [13], there was enough time for the activity of twinning and detwinning to modify local grain orientations and that could favor the activation of some slip systems.

For polycrystalline material, plastic deformation within grains tends to be constrained by neighboring grains. However, grains near specimen surface are partly surrounded by free surface which makes it easier for material transfer, and that could lead to surface roughing or near surface structure change. Since plastic deformation is easier near the specimen surface, the aforementioned three mechanisms concerning about twinning-involved fatigue damage process could lead to more severe damage around the specimen surface or near surface.

In addition, the conventional cyclic slip and environmental effects could further accelerate the fatigue damage process around the specimen surface or near surface areas. As we know, fatigue damage is a complex process. We agree with the idea that cyclic slip mechanisms or environmental effects play important roles in different alloys, but in the present study we emphasize the specialty of twinning-involved fatigue damage mechanisms in our investigated AZ31 alloy.

Based on the discussion above, cyclic deformation irreversibility caused by twinning is one crucial factor influencing the fatigue property of extruded AZ31 magnesium alloy. It was proposed that decreasing grain size to certain level would lead to a transition of dominant deformation mode from twinning to slip [20]. Thus, it is assumed that refining grain size could simultaneously increase the material's strength due to the well-known Hall-Patch law and reduces the cyclic deformation irreversibility for extruded AZ31 magnesium alloy with certain deformation textures, which could be an effective way for improving the fatigue properties.

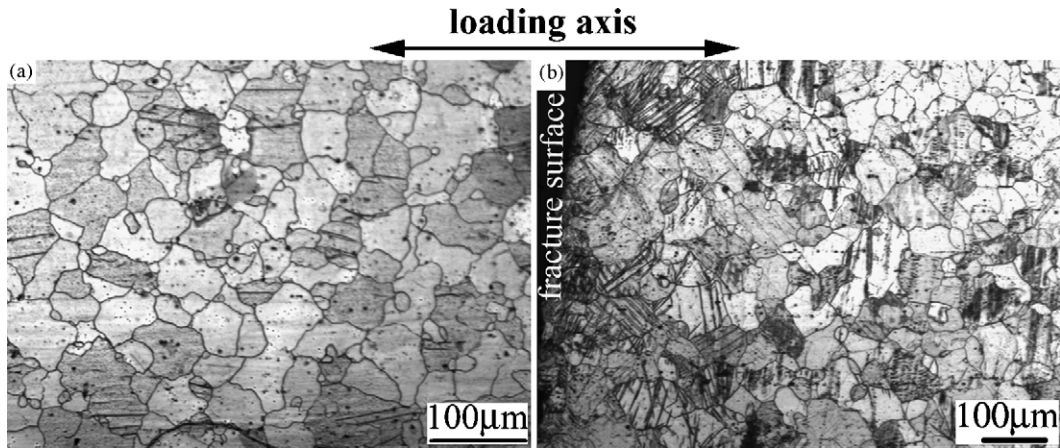


Fig. 5. Optical images of microstructures on the specimen section parallel to the gauge length (a) before and (b) after ultrasonic fatigue testing, respectively; (b) the area right below the fracture surface. Loading axis direction was marked.

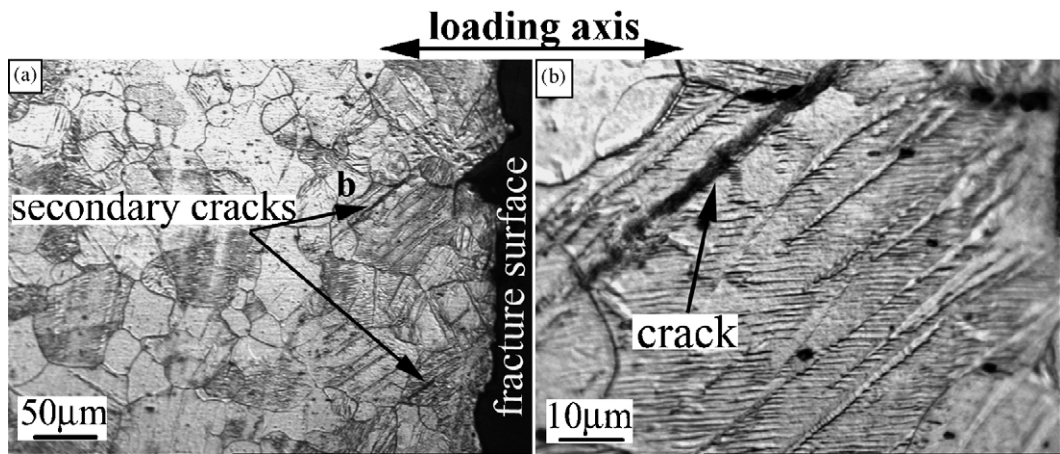


Fig. 6. Optical images of the specimen section parallel to the gauge length beneath the fracture surface (ultrasonic fatigue,  $\pm 100$  MPa,  $1.032 \times 10^8$  cycles): (a) secondary cracks formed along twin bands; (b) magnified image of the crack marked b in (a). Loading axis direction was marked.

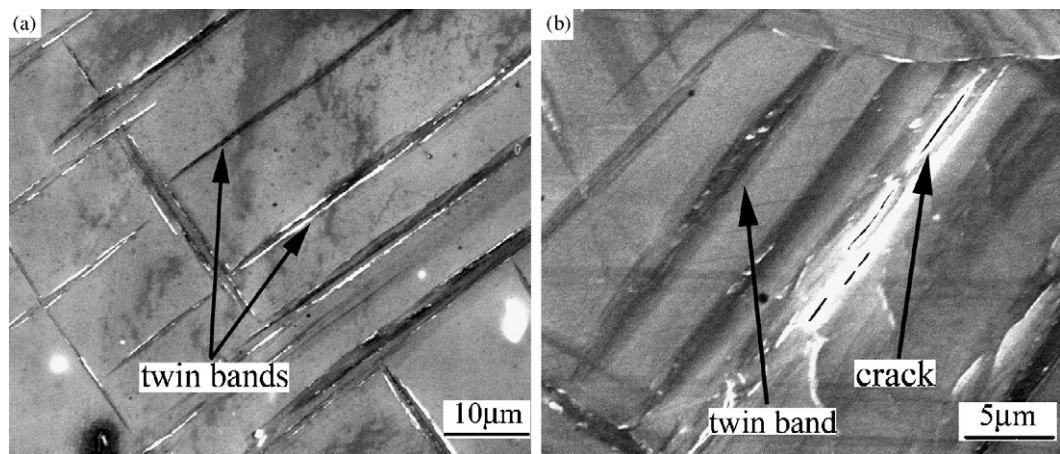


Fig. 7. SEM images of specimen surface after conventional fatigue loading: (a) deformation twins were visible after  $10^4$  cycles (conventional fatigue,  $\pm 90$  MPa); (b) microcracks were found to initiate along twin bands after further fatigue under  $\pm 120$  MPa as indicated by arrow.

#### 4. Conclusions

The fatigue behavior in the very high cycle regime of extruded AZ31 magnesium alloy has been studied. Cyclic failure mainly

originated from the surface or near surface of specimens with the  $S-N$  curve appearing in a continuous decreasing trend. Moderate fatigue ratio ( $\sigma_{-1}/\sigma_b$ ) for AZ31 at  $10^9$  cycles was observed. Fatigue cracks were observed along twin bands. Twinning-

involved cyclic deformation irreversibility was active in the fatigue damage process, which was considered as one specific mechanism of crack initiation among others in the present alloy. Grain refinement was suggested as one potential way for improving fatigue properties of some wrought magnesium alloys with certain textures.

### Acknowledgements

This work was supported by National Natural Science Foundation of China (NSFC) under grant No. 50471082. Zhang Z.F. would like to acknowledge the financial support of “Hundred of Talents Project” by Chinese Academy of Sciences and the National Outstanding Young Scientist Foundation under grant No. 50625103.

### References

- [1] Z.B. Sajuri, Y. Miyashita, Y. Hosokai, Y. Mutoh, *Int. J. Mech. Sci.* 48 (2006) 198–209.
- [2] C. Potzies, K.U. Kainer, *Adv. Eng. Mater.* 6 (2004) 281–289.
- [3] H. Mayer, H.J. Lipowsky, M. Papakyriacou, R. Rösch, A. Stich, S. Stanzl-Tschegg, *Fatigue Fract. Eng. Mater. Struct.* 22 (1999) 591–599.
- [4] H. Mayer, M. Papakyriacou, B. Zettl, S. Stanzl-Tschegg, *Int. J. Fatigue* 25 (2003) 245–256.
- [5] D.K. Xu, L. Liu, Y.B. Xu, E.H. Han, *Scripta Mater.* 56 (2007) 1–4.
- [6] T.S. Shih, W.S. Liu, Y.J. Chen, *Mater. Sci. Eng. A* 325 (2002) 152–162.
- [7] K. Tokaji, M. Kamakura, Y. Ishiizumi, N. Hasegawa, *Int. J. Fatigue* 26 (2004) 1217–1224.
- [8] G.L. Song, A. Atrens, *Adv. Eng. Mater.* 1 (1999) 11–33.
- [9] S. Kleiner, P.J. Uggowitzer, *Mater. Sci. Eng. A* 379 (2004) 258–263.
- [10] L. Jiang, J.J. Jonas, A.A. Luo, A.K. Sachdev, S. Godet, *Scripta Mater.* 54 (2006) 771–775.
- [11] H. Mayer, *Int. Mater. Rev.* 44 (1999) 1–34.
- [12] V.V. Ogarrevic, R.I. Stephens, *Annu. Rev. Mater. Sci.* 20 (1990) 141–177.
- [13] Q.Y. Wang, C. Bathias, N. Kawagoishi, Q. Chen, *Int. J. Fatigue* 24 (2002) 1269–1274.
- [14] H. Mughrabi, *Fatigue Fract. Eng. Mater. Struct.* 22 (1999) 633–641.
- [15] H. Mughrabi, *Int. J. Fatigue* 28 (2006) 1501–1508.
- [16] Y.N. Wang, J.C. Huang, *Acta Mater.* 55 (2007) 897–905.
- [17] R. Stevenson, J.B. Vander Sande, *Acta Metall.* 22 (1974) 1079–1086.
- [18] X.L. Tan, H.C. Gu, *Int. J. Fatigue* 18 (1996) 329–333.
- [19] H. Li, Q.Q. Duan, X.W. Li, Z.F. Zhang, *Mater. Sci. Eng. A* 466 (2007) 38–46.
- [20] M.R. Barnett, Z. Keshavarz, A.G. Beer, D. Atwell, *Acta Mater.* 52 (2004) 5093–5103.